

Effects of noise on synchronization in simplicial complexes

Linying Xiang(项林英), Shuwei Yao(姚姝玮), Yining Chen(陈艺宁), Ruitong Yan(闫锐桐), and Ruya Xia(夏儒雅)
Citation: Chin. Phys. B, 2025, 34 (**7**): 070503. DOI: 10.1088/1674-1056/adc7ef
Journal homepage: http://cpb.iphy.ac.cn; http://iopscience.iop.org/cpb

What follows is a list of articles you may be interested in

Synchronous dynamics of robotic arms driven by Chua circuits

Guoping Sun(孙国平), Mingxin Xu(许明鑫), Guoqiang Jin(金国强), and Xufeng Wang(王旭峰)
Chin. Phys. B, 2025, 34 (**6**): 060501. DOI: 10.1088/1674-1056/adc2e1

Effects of potential field delay and coupling delay on collective behavior of a fractional-order coupled system in a dichotomous fluctuating potential

Yangfan Zhong(钟扬帆), Xi Chen(陈熙), Maokang Luo(罗懋康), and Tao Yu(蔚涛)
Chin. Phys. B, 2025, 34 (**5**): 050501. DOI: 10.1088/1674-1056/adbd15

Effects of asymmetric coupling and boundary on the dynamic behaviors of a random nearest neighbor coupled system

Ling Xu(徐玲) and Lei Jiang(姜磊)
Chin. Phys. B, 2024, 33 (**6**): 060503. DOI: 10.1088/1674-1056/ad3b86

Dynamics and synchronization of neural models with memristive membranes under energy coupling

Jingyue Wan(万婧玥), Fuqiang Wu(吴富强), Jun Ma(马军), and Wenshuai Wang(汪文帅)
Chin. Phys. B, 2024, 33 (**5**): 050504. DOI: 10.1088/1674-1056/ad1dcc

Chimera states of phase oscillator populations with nonlocal higher-order couplings

Yonggang Wu(伍勇刚), Huajian Yu(余华健), Zhigang Zheng(郑志刚), and Can Xu(徐灿)
Chin. Phys. B, 2024, 33 (**4**): 040504. DOI: 10.1088/1674-1056/ad1481

Effects of noise on synchronization in simplicial complexes

Linying Xiang(项林英)[1,†], Shuwei Yao(姚姝玮)[1], Yining Chen(陈艺宁)[1], Ruitong Yan(闫锐桐)[1], and Ruya Xia(夏儒雅)[2]

[1] *School of Artificial Intelligence, Tiangong University, Tianjin* 300387, *China*
[2] *School of Control Engineering, Northeastern University at Qinhuangdao, Qinhuangdao* 066004, *China*

(Received 14 January 2025; revised manuscript received 19 March 2025; accepted manuscript online 2 April 2025)

This paper explores the synchronization of stochastic simplicial complexes with noise, modeled by stochastic differential equations of Itô type. It establishes the relationship between synchronization and individual dynamics, higher-order structures, coupling strengths, and noise. In particular, this study delves into the role of multi-body interactions, particularly focusing on the influence of higher-order simplicial structures on the overall synchronization behavior. Furthermore, the effects of noise on synchronizability in the stochastic simplicial complex are thoroughly examined. The obtained results indicate that the effects of noise on the synchronizability vary with the manner in which noise propagates. The presence of noise can regulate the synchronization pattern of the simplicial complex, transforming the unstable state into a stable state, and vice versa. These findings offer valuable insights and a theoretical foundation for improving the performance of real-world networks, such as communication networks, biological systems, and social networks, where noise is often inevitable.

Keywords: simplical complex, higher-order network, synchronization, noise, stochastic differential equation

PACS: 05.45.Xt, 05.45.–a

DOI: 10.1088/1674-1056/adc7ef **CSTR:** 32038.14.CPB.adc7ef

1. Introduction

Many real-world complex systems can be effectively modeled as networks where nodes interact with each other.[1–3] Over the past two decades, the study of synchronization in complex networks has become a central topic in network science and control engineering.[4–13] Most previous research on network synchronization has focused on pairwise interactions represented by edges between nodes. Recently, there has been growing interest in higher-order interactions in networks.[14–27] Higher-order networks represent a more advanced and detailed framework for modeling complex systems compared to traditional first-order networks. These networks capture not only pairwise relationships between nodes but also interactions involving multiple entities simultaneously, which can lead to a more accurate representation of systems where higher-level dependencies exist.[28–36] In computational neuroscience, high-order networks have been applied to model the complex interactions between different regions of the brain.[24] For instance, rather than just considering direct connections between two brain regions (as in traditional network analysis), high-order networks incorporate interactions involving three or more brain regions at the same time, which can reveal more intricate patterns of neural activity. This can be crucial for understanding neurological diseases such as Alzheimer's or epilepsy. Given the ubiquity of higher-order structures in real-world systems, such as social networks, ecosystems, and the human brain, it is both theoretically and practically significant to explore the synchronization of higher-order networks.

Simplicial complexes serve as effective topological tools for representing higher-order interactions among nodes.[37] In Ref. [28], a comprehensive framework for the dynamics of simplicial complexes was proposed, with a specific focus on the stability of synchronization. Building upon this framework, studies have extended to multi-layer higher-order networks[29] and directed higher-order networks,[30] using the master stability function (MSF) approach to analyze synchronization in simplicial complexes.[31] In Ref. [33], the authors demonstrated that simplicial complexes are powerful tools for capturing and reflecting the complexities of higher-order interactions of nodes.

In real-world applications, nearly all networked systems are subject to random uncertainties such as stochastic forces and noisy measurements.[12,38–42] Therefore, networks perturbed by noise have attracted the interest of researchers.[44,45] In particular, the authors in Ref. [44] has demonstrated that the presence of noise not only leads to the transition of firing patterns, but also achieves the phase synchronization between two heterogeneous neurons under low coupling strength. It has also been found that increasing noise intensity might enhance synchronization when the noise affects all state variables.[46,47] However, there has been no systematic study on the impact of noise on synchronization in simplicial complexes. Given the complexity and prevalence of noise in prac-

[†]Corresponding author. E-mail: xianglinying@tiangong.edu.cn

© 2025 Chinese Physical Society and IOP Publishing Ltd. All rights, including for text and data mining, AI training, and similar technologies, are reserved.

tical systems, investigating its influence on the synchronization of simplicial complexes is crucial. Most existing studies focus on pairwise interactions in simple networks, leaving a gap in understanding the effects of noise in more complex, higher-order networks. Simplicial complexes, with their ability to model multi-body interactions, offer a richer structure to explore noise-driven dynamics. These interactions, which extend beyond the traditional node-to-node connections, introduce additional challenges and opportunities for synchronization analysis, particularly when noise is present. In this context, noise can propagate through simplicial complexes in different ways, depending on the structure and strength of the interactions between nodes and simplices. The introduction of stochasticity in these systems raises new questions about how synchronization stability is affected by higher-order interactions and whether existing methods, like the MSF approach, can be adapted to handle these complexities.

Motivated by the discussions above, this paper investigates the synchronization issue in stochastic simplicial complexes with noise. By extending previous work on noise-induced synchronization and applying it to higher-order structures, we seek to provide a deeper understanding of how noise influences the stability and performance of real-world networks modeled as simplicial complexes. Our work also aims to fill the gap in the literature by offering new insights into the interplay between noise, coupling strengths, and higher-order interactions in the context of complex networked systems.

The main contributions of this paper can be summarized as follows. First, it analyzes and discusses the local stability of synchronization in stochastic simplicial complexes, establishing the relationship between synchronization and various factors such as individual dynamics, higher-order structures, coupling strengths, and noise. Building upon the MSF framework, an extended master stability equation is derived, leading to a novel MSF formulation that incorporates noise, distinguishing it from commonly used network models. The significance of this research lies in its exploration of higher-order interactions in complex systems, extending beyond the traditional pairwise interactions often studied in network theory. Simplicial complexes provide a natural framework to model such higher-order structures, capturing interactions between groups of nodes, such as triangles (3-body interactions) and higher-dimensional structures, which are common in many real-world networks like brain networks, social networks, and power grids. Additionally, the incorporation of stochastic effects introduces a layer of realism, as noise is inevitable in practical systems. The study investigates how different noise propagation mechanisms — whether through nodes, edges, or higher-dimensional structures — impact the system's ability to achieve synchronization. The findings suggest that the topology of the simplicial complex and the way noise is introduced can significantly affect the overall robustness and stability of synchronization. It reveals that when noise diffuses through all state variables, synchronizability can be enhanced by appropriately increasing noise intensity. However, under different network parameter configurations, noise may have varying effects: sometimes beneficial, and other times detrimental. These insights are particularly relevant for the design and optimization of engineered systems, such as autonomous vehicle networks, distributed sensor networks, and neural networks, where reliable synchronization is critical. By understanding how noise and higher-order interactions influence synchronizability, this work provides guidelines for developing more robust and resilient systems capable of maintaining synchronization even under noisy and dynamic conditions. Moreover, it offers a theoretical foundation for future research in both the mathematical modeling of complex systems and the application of these principles to real-world problems.

The rest of this paper is organized as follows. Section 2 introduces relevant preliminaries, including the basic definitions and properties of simplicial complexes. Section 3 analyzes and discusses the local stability of synchronization in stochastic simplicial complexes. This section provides a detailed examination of the synchronization conditions, derived from the extended MSF approach, for simplicial complexes with noise. Section 4 examines the effects of noise on synchronizability. Specifically, we investigate how different noise propagation mechanisms influence the synchronizability of simplicial complexes. Section 5 concludes the paper, summarizing the key findings and contributions of this work, and also outlining potential future research directions.

2. Preliminaries

2.1. Notation

Let $\mathbb{R}$ denote the set of real numbers, $\mathbb{R}^n$ the set of n-dimensional real vectors, and $\mathbb{R}^{n\times m}$ the set of $n\times m$ real matrices. The symbol $\otimes$ represents the Kronector product, $d!$ denotes the factorial of d, defined as the product of all positive integers from 1 to d, and $\lambda(A)$ denotes the set of eigenvalues of the matrix A. I_N represents an $N\times N$ identity matrix and $\mathrm{diag}\,(b_1,b_2,\ldots,b_N)$ denotes an $N\times N$ diagonal matrix with diagonal elements $b_1,b_2,\ldots,b_N$.

2.2. Simplicial complexes

A simplex is a mathematical structure suitable for expressing higher-order interactions. In an undirected graph, a d-simplex corresponds to a complete graph with $d+1$ nodes. In this paper, a d-simplex is employed to model the structure of $(d+1)$-body interactions involving $d+1$ nodes. A simplicial complex is composed of simplexes of different dimensions. Figure 1 illustrates an example of a simplicial complex. For

each dimension d, where $d = 1,2,\ldots,D$, the adjacency tensor $A^{(d)} = (a^{(d)}_{i_1 i_2 \ldots i_{d+1}})$ is an $N \times N \times \ldots \times N|_{d+1}$ tensor, where $a^{(d)}_{i_1 i_2 \ldots i_{d+1}} = 1$ if the d-simplex $(i_1, i_2, \ldots, i_{d+1})$ belongs to a simplicial complex, and $a^{(d)}_{i_1 i_2 \ldots i_{d+1}} = 0$ otherwise.[27] Furthermore, the generalized d-degree $k^{(d)}_i$ of the i-th node is defined as[28]

$$k^{(d)}_i = \frac{1}{d!} \sum_{i_1=1}^{N} \sum_{i_2=1}^{N} \cdots \sum_{i_d=1}^{N} a^{(d)}_{i i_1 i_2 \ldots i_d}, \quad i = 1,2,\ldots,N. \tag{1}$$

The generalized d-degree $k^{(d)}_{ij}$ of an edge (v_i, v_j) is defined as

$$k^{(d)}_{ij} = \frac{1}{(d-1)!} \sum_{i_1=1}^{N} \sum_{i_2=1}^{N} \cdots \sum_{i_{d-1}=1}^{N} a^{(d)}_{iji_1 i_2 \ldots i_{d-1}}, \quad i = 1,2,\ldots,N. \tag{2}$$

The generalized Laplacian $L^{(d)}$ of order d, with $d = 1,2,\ldots,D$, are defined as

$$L^{(d)}_{ij} = \begin{cases} 0, & a^{(1)}_{ij} = 0, \ i \neq j, \\ -(d-1)!k^{(d)}_{ij}, & a^{(1)}_{ij} = 1, \ i \neq j, \\ d!k^{(d)}_i, & i = j, \end{cases} \quad i = 1,2,\ldots,N. \tag{3}$$

It is evident that all generalized Laplacians $L^{(d)}$, $d = 1,2,\ldots,D$, are real symmetric matrices with zero row sums.

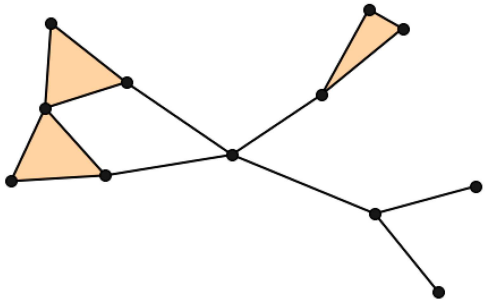


Fig. 1. An example of a simplicial complex.

Note that the generalized degree plays an essential role in characterizing the topological features of the simplicial complex at different dimensions. The adjacency tensor $A^{(d)}$ allows us to extend traditional graph theory concepts, such as connectivity and centrality, to higher-order structures, capturing more complex interactions between nodes beyond pairwise connections. Moreover, the higher-order generalized Laplacian matrices associated with simplicial complexes are crucial for analyzing the dynamics on such structures. These Laplacians, constructed from the adjacency tensors of different dimensions, provide a foundation for studying synchronization, diffusion, and other processes in networks with multi-body interactions. By considering both the topological and dynamical aspects of simplicial complexes, we can develop a deeper understanding of how higher-order interactions influence the behavior of complex systems, particularly in the presence of noise or other perturbations.

3. Synchronization of stochastic simplicial complexes

Consider a general D-dimensional stochastic simplical complex consisting of N identical nodes with nonlinear dynamics, described by

$$\begin{aligned} \mathrm{d}x_i = & \Bigg(F(x_i) + \sigma_1 \sum_{j_1=1}^{N} a^{(1)}_{ij_1} H^{(1)}(x_i, x_{j_1}) \\ & + \sigma_2 \sum_{j_1=1}^{N} \sum_{j_2=1}^{N} a^{(2)}_{ij_1 j_2} H^{(2)}(x_i, x_{j_1}, x_{j_2}) + \cdots \\ & + \sigma_D \sum_{j_1=1}^{N} \cdots \sum_{j_D=1}^{N} a^{(D)}_{ij_1 \ldots j_D} H^{(D)}(x_i, x_{j_1}, \ldots, x_{j_D}) \Bigg) \mathrm{d}t \\ & + \sigma_v g(x_i)\, \mathrm{d}W(t), \quad i = 1,2,\ldots,N, \end{aligned} \tag{4}$$

where $x_i = [x_{i1}, x_{i2}, \ldots, x_{im}]^{\mathrm{T}} \in \mathbb{R}^m$ is the state vector of node i, $F(\cdot)$: $\mathbb{R}^m \to \mathbb{R}^m$ is a continuously differentiable nonlinear function describing the self-dynamics of each node, and $H^{(d)}$: $\mathbb{R}^{(d+1)m} \to \mathbb{R}^m$ $(d = 1,2,\ldots,D)$ are synchronization non-invasive inner-coupling functions $(H^{(d)}(x,x,\ldots,x) \equiv 0, \forall d)$, describing the coupling forms at different orders. The parameters $\sigma_d \in \mathbb{R}$ $(d = 1,2,\ldots,D)$ are assumed to be positive, describing the coupling strengths. Moreover, $a^{(d)}_{ij_1 \ldots j_d}$ are the entries of the adjacency tensors $A^{(d)}$, $d = 1,2,\ldots,D$. The stochastic term $\sigma_v g(x_i)\, \mathrm{d}W(t)$ describes uncertainties in the individual dynamics, where $W(t)$ is a standard Brownian motion, $g(\cdot) : \mathbb{R}^m \to \mathbb{R}^m$ is the diffusion function describing how the Brownian motion propagates on each node, and σ_v is the noise intensity.

Notice that the network described by Eq. (4) is a nonlinear stochastic differential equation of Itô type. To provide a clearer and more general description, we analyze the case of $D = 2$ in the following. It should be noted that all the analyses conducted for $D = 2$ can be extended to higher orders $D > 2$.

When $D = 2$, equation (4) can be rewritten as

$$\begin{aligned} \mathrm{d}x_i = & \Bigg(F(x_i) + \sigma_1 \sum_{j_1=1}^{N} a^{(1)}_{ij_1} H^{(1)}(x_i, x_{j_1}) \\ & + \sigma_2 \sum_{j_1=1}^{N} \sum_{j_2=1}^{N} a^{(2)}_{ij_1 j_2} H^{(2)}(x_i, x_{j_1}, x_{j_2}) \Bigg) \mathrm{d}t \\ & + \sigma_v g(x_i)\, \mathrm{d}W(t), \quad i = 1,2,\ldots,N, \end{aligned} \tag{5}$$

where σ_1 and σ_2 are the coupling strengths associated with two-body and three-body interactions, respectively.

The objective is to achieve synchronization of the stochastic simplicial complex given by Eq. (5) to a desired state x_{s}, which satisfies

$$\mathrm{d}x_{\mathrm{s}} = F(x_{\mathrm{s}})\mathrm{d}t + \sigma_v g(x_{\mathrm{s}})\mathrm{d}W(t). \tag{6}$$

In this paper, the following inner-coupling functions are considered.

Assumption 1 Suppose that the forms of inner-coupling functions are described by[28]

$$\begin{aligned} H^{(1)}(x_i,x_j) &= \omega^{(1)}(x_j) - \omega^{(1)}(x_i), \\ H^{(2)}(x_i,x_j,x_k) &= \omega^{(2)}(x_j,x_k) - \omega^{(2)}(x_i,x_i), \end{aligned} \tag{7}$$

where $\omega^{(d)}$, $d = 1,2,\ldots,D$: $\mathbb{R}^{dm} \to \mathbb{R}^m$ satisfy the following condition:

$$\omega^{(2)}(x,x) = \omega^{(1)}(x). \tag{8}$$

The stability condition for synchronization is formulated as follows:

Theorem 1 Suppose Assumption 1 holds. The stochastic simplicial complex (5) achieves synchronization if $\Lambda < 0$, where Λ is the largest Lyapunov exponent calculated by the extended master stability equation.

The synchronized region $\mathbb{S}$ is defined as the set of values of η for which $\Lambda = \Lambda(\eta,\sigma_v) < 0$. Here, $\Lambda(\eta,\sigma_v)$ is referred to as the MSF of the extended master stability equation (see Appendix A). Note that the extended MSF mentioned above incorporates noise, distinguishing it from commonly used network models. The boundary curve of the synchronized region is determined by the largest Lyapunov exponent.

4. Effects of noise on synchronization

In this section, we discuss the effects of noise on the synchronization of the stochastic simplicial complexes composed of Van der Pol oscillators and Rössler systems, respectively. We begin by examining the dynamics of these two systems under different noise propagation mechanisms applied to simplicial complexes of various dimensions.

For the Van der Pol oscillators, which exhibit limit cycle behavior, we investigate how noise impacts the synchronization of nodes in simplices of different orders. We focus on how the coupling strength and noise intensity affect the stability of synchronization, particularly when the oscillators are subject to external stochastic forces. By adjusting the noise intensity and exploring the role of multi-body interactions, we aim to determine the critical thresholds beyond which synchronization is either enhanced or disrupted. Numerical simulations are provided to illustrate the noise-induced synchronization and its dependence on the topology of the simplicial complex.

For the Rössler systems, which display chaotic dynamics, the analysis is extended to explore how the interplay between chaotic behavior and stochastic perturbations influences the overall synchronizability of the simplicial complex. In particular, we assess the effects of noise on the long-term synchronization behavior of higher-order interactions, focusing on the synchronization of chaotic attractors under different levels of noise intensity. The analysis shows that, while moderate noise may enhance synchronization through stochastic resonance, excessive noise can lead to desynchronization and instability.

4.1. Van der Pol oscillator

A Van der Pol oscillator is described by

$$\begin{aligned} \dot{x}_{i1} &= x_{i2}, \\ \dot{x}_{i2} &= \mu(1-x_{i1}^2)x_{i2} - x_{i1}, \end{aligned} \tag{9}$$

where $\mu = 0.2$. The corresponding Jacobian matrix J_{F} is given by

$$J_{\mathrm{F}} = \begin{bmatrix} 0 & 1 \\ -2\mu x_{s1}x_{s2} - 1 & \mu(1-x_{s1}^2) \end{bmatrix}. \tag{10}$$

Next, the J_g under different diffusion functions is provided.

(i) Consider the case where the diffusion function $g(x_i) = x_i$. This means that the noise diffuses to all state variables of the nodes. Then

$$J_g = \begin{bmatrix} 1 & 0 \\ 0 & 1 \end{bmatrix}. \tag{11}$$

The desired state $x_{\mathrm{s}} = [x_{s1},x_{s2}]^{\mathrm{T}}$ satisfies the following condition:

$$\begin{bmatrix} \mathrm{d}x_{s1} \\ \mathrm{d}x_{s2} \end{bmatrix} = \begin{bmatrix} x_{s2} \\ \mu(1-x_{s1}^2)x_{s2} - x_{s1} \end{bmatrix} \mathrm{d}t + \sigma_v \begin{bmatrix} x_{s1} \\ x_{s2} \end{bmatrix} \mathrm{d}W(t). \tag{12}$$

(ii) Consider the case where the diffusion function $g(x_i) = [x_{i1},0]^{\mathrm{T}}$, implying that the noise only affects the first state variable of the node. Then

$$J_g = \begin{bmatrix} 1 & 0 \\ 0 & 0 \end{bmatrix}. \tag{13}$$

Therefore, the desired state x_{s} satisfies the following condition:

$$\begin{bmatrix} \mathrm{d}x_{s1} \\ \mathrm{d}x_{s2} \end{bmatrix} = \begin{bmatrix} x_{s2} \\ \mu(1-x_{s1}^2)x_{s2} - x_{s1} \end{bmatrix} \mathrm{d}t + \sigma_v \begin{bmatrix} x_{s1} \\ 0 \end{bmatrix} \mathrm{d}W(t). \tag{14}$$

(iii) Consider the case where the diffusion function $g(x_i) = [0,x_{i2}]^{\mathrm{T}}$. This indicates that the noise affects only the second state variable of the node. Then

$$J_g = \begin{bmatrix} 0 & 0 \\ 0 & 1 \end{bmatrix}. \tag{15}$$

The desired state x_{s} satisfies the following condition:

$$\begin{bmatrix} \mathrm{d}x_{s1} \\ \mathrm{d}x_{s2} \end{bmatrix} = \begin{bmatrix} x_{s2} \\ \mu(1-x_{s1}^2)x_{s2} - x_{s1} \end{bmatrix} \mathrm{d}t + \sigma_v \begin{bmatrix} 0 \\ x_{s2} \end{bmatrix} \mathrm{d}W(t). \tag{16}$$

Next, the $J_{\omega^{(1)}}$ under different inner-coupling functions is provided.

(I) Consider the case where $\omega^{(1)}(x_j) = [x_{j1}^3,0]^{\mathrm{T}}$ and $\omega^{(2)}(x_j,x_k) = [x_{j1}^2x_{k1},0]^{\mathrm{T}}$. The Jacobian matrix $J_{\omega^{(1)}}$ is given by

$$J_{\omega^{(1)}} = \begin{bmatrix} 3x_{s1}^2 & 0 \\ 0 & 0 \end{bmatrix}. \tag{17}$$

(II) Consider the case where $\omega^{(1)}(x_j) = [x_{j1}^3, x_{j2}^3]^{\mathrm{T}}$ and $\omega^{(2)}(x_j, x_k) = [x_{j1}^2 x_{k1}, x_{j2}^2 x_{k2}]^{\mathrm{T}}$. The Jacobian matrix $J_{\omega^{(1)}}$ is given by

$$J_{\omega^{(1)}} = \begin{bmatrix} 3x_{s1}^2 & 0 \\ 0 & 3x_{s2}^2 \end{bmatrix}. \tag{18}$$

Note that equations (10)–(18) will be utilized to compute the largest Lyapunov exponent of the extened MSF given in Eq. (A8) in Appendix A. In what follows, we discuss the influence of noise on the synchronization of the stochastic simplicial complex of Van der Pol oscillators.

Figure 2 illustrates the largest Lyapunov exponents $\Lambda(\eta, \sigma_v)$ under different values of η and σ_v. Figure 2(a) corresponds to the case where the inner-coupling functions are $\omega^{(1)}(x_j) = [x_{j1}^3, 0]^{\mathrm{T}}$ and $\omega^{(2)}(x_j, x_k) = [x_{j1}^2 x_{k1}, 0]^{\mathrm{T}}$, and the diffusion function is $g(x_i) = x_i$. In Figs. 2(a), 6(a), 7(a), and 8(a) below, the regions where $\Lambda < 0$ are shaded in green, while $\Lambda > 0$ are shaded in red. It is observed that increasing noise intensity expands the synchronized region, suggesting that noise can enhance synchronization in the stochastic simplicial complex when it affects all state variables. This observation is reinforced by Fig. 2(b), which presents MSF curves under different noise intensities $\sigma_v = 0.2$, 0.8, 1.2, 2. Specifically, at $\sigma_v = 0.2$, the largest Lyapunov exponent approaches 30, while at $\sigma_v = 0.8$, it starts to decrease towards 0. With further increase to $\sigma_v = 1.2$, the MSF curve dips below 0, indicating potential for achieving synchronization in the stochastic simplicial complex.

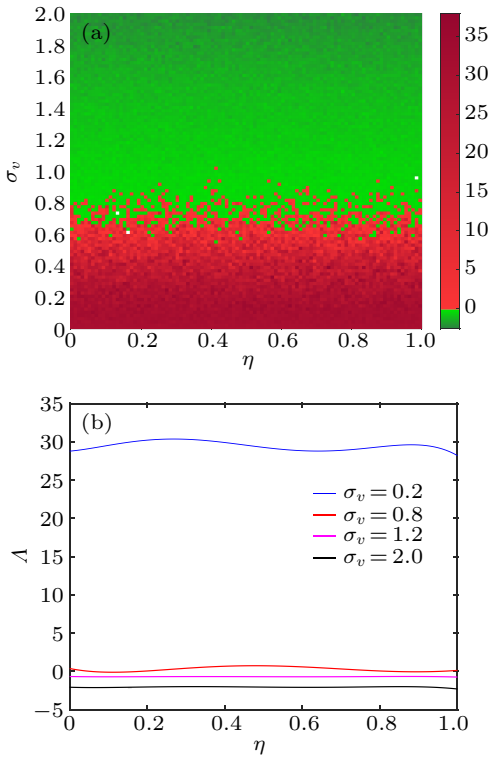


Fig. 2. The stochastic simplicial complex of Van der Pol oscillators with $g(x_i) = x_i$, $\omega^{(1)}(x_j) = [x_{j1}^3, 0]^{\mathrm{T}}$, and $\omega^{(2)}(x_j, x_k) = [x_{j1}^2 x_{k1}, 0]^{\mathrm{T}}$: (a) the largest Lyapunov exponents $\Lambda(\eta, \sigma_v)$, (b) the MSF curves for different noise intensities.

In what follows, we consider a simplicial complex of four nodes, which has two 2-simplex, as shown in Fig. 3. Set $\sigma_1 = \sigma_2 = 1$. The evolution of the node states with Van der Pol oscillators under $\sigma_v = 0.1$ and 2 are illustrated in Figs. 4(a) and 4(b), respectively. It can be observed that the simplicial complex is unstable under $\sigma_v = 0.1$, while becomes stable under $\sigma_v = 2$ at the desired state. The corresponding system errors are illustrated in Figs. 5(a) and 5(b), respectively. The simulated results are in good agreement with the results in Fig. 2. It demonstrates that the presence of noise can regulate the synchronization pattern of the simplicial complex, transforming the unstable state into a stable state.

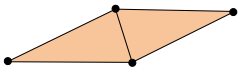


Fig. 3. A simplicial complex of four nodes.

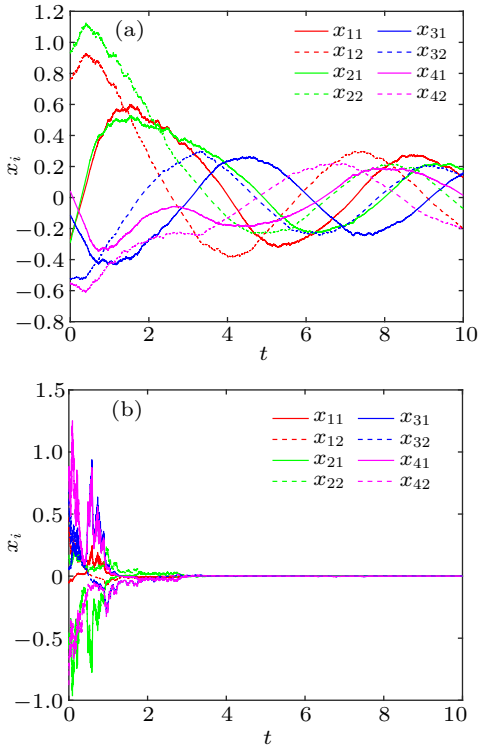


Fig. 4. The evolution of the node states with Van der Pol oscillators under different noise intensities: (a) $\sigma_v = 0.1$ and (b) $\sigma_v = 2$.

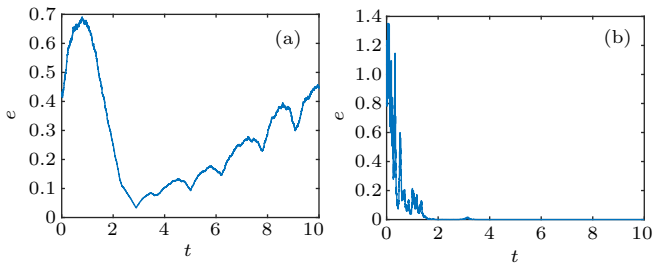


Fig. 5. The evolution of the system errors with Van der Pol oscillators under different noise intensities: (a) $\sigma_v = 0.1$ and (b) $\sigma_v = 2$.

Figure 6(a) depicts the largest Lyapunov exponents $\Lambda(\eta, \sigma_v)$ under varying η and σ_v. Specifically, figure 6(a) considers the scenario where the inner-coupling functions are

$\omega^{(1)}(x_j) = [x_{j1}^3, x_{j2}^3]^{\mathrm{T}}$ and $\omega^{(2)}(x_j, x_k) = [x_{j1}^2 x_{k1}, x_{j2}^2 x_{k2}]^{\mathrm{T}}$, and the diffusion function is $g(x_i) = x_i$. Similar to Fig. 2(a), the synchronized region expands with increasing noise intensity, indicating that noise can enhance synchronization in the stochastic simplicial complex.

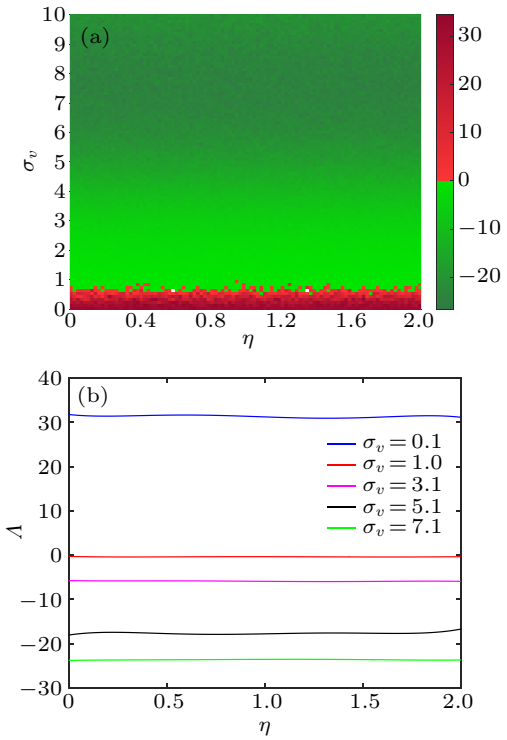


Fig. 6. The stochastic simplicial complex of Van der Pol oscillators with $g(x_i) = x_i$, $\omega^{(1)}(x_j) = [x_{j1}^3, x_{j2}^3]^{\mathrm{T}}$, and $\omega^{(2)}(x_j, x_k) = [x_{j1}^2 x_{k1}, x_{j2}^2 x_{k2}]^{\mathrm{T}}$: (a) the largest Lyapunov exponents $\Lambda(\eta, \sigma_v)$, (b) the MSF curves for different noise intensities.

From the above analysis, we can conclude that increasing the noise intensity can enhance the synchronizability of the stochastic simplicial complex, provided that the noise diffuses through all variables of the nodes. This phenomenon, often referred to as stochastic resonance, indicates that a moderate level of noise can help the system to synchronize more effectively by mitigating the effects of small perturbations and stabilizing the collective dynamics. However, it is crucial to note that this enhancement in synchronizability is highly dependent on how the noise propagates through the system. In particular, when noise affects all state variables of each node uniformly, the increased randomness helps the system to overcome local instabilities and reach global synchronization more efficiently. Conversely, when noise is selectively applied to only a subset of the node's state variables, the effect on synchronizability becomes less predictable and may lead to destabilization, depending on the specific interaction dynamics and the network's higher-order structures. This will be validated through the following examples.

Next, consider the scenario where $\omega^{(1)}(x_j) = [x_{j1}^3, 0]^{\mathrm{T}}$, $\omega^{(2)}(x_j, x_k) = [x_{j1}^2 x_{k1}, 0]^{\mathrm{T}}$, and $g(x_i) = [x_{i1}, 0]^{\mathrm{T}}$. Unlike in Figs. 2 and 6, figure 7(a) demonstrates that the synchronized region emerges only when σ_v is sufficiently large; however, if the noise intensity becomes too high, the synchronized

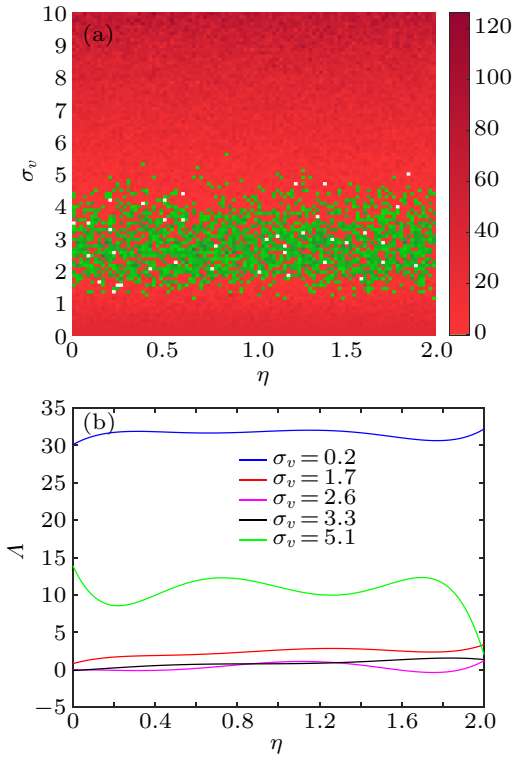


Fig. 7. The stochastic simplicial complex of Van der Pol oscillators with $g(x_i) = [x_{i1}, 0]^{\mathrm{T}}$, $\omega^{(1)}(x_j) = [x_{j1}^3, 0]^{\mathrm{T}}$, and $\omega^{(2)}(x_j, x_k) = [x_{j1}^2 x_{k1}, 0]^{\mathrm{T}}$: (a) the largest Lyapunov exponents $\Lambda(\eta, \sigma_v)$, (b) the MSF curves for different noise intensities.

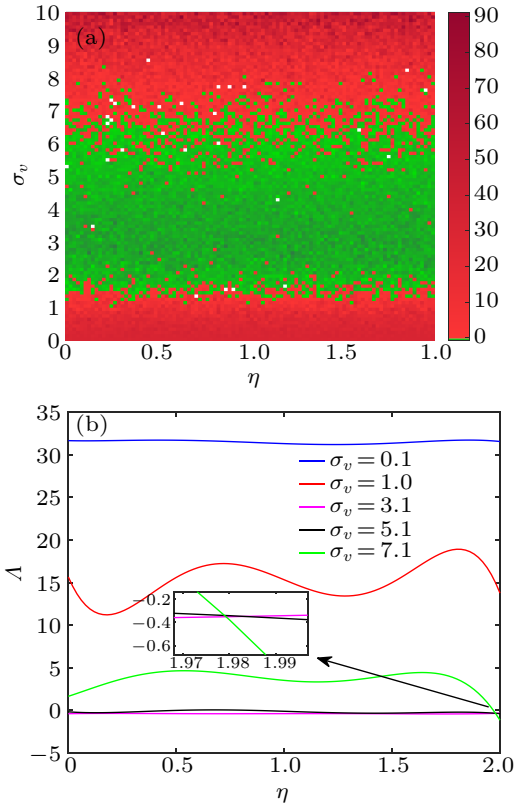


Fig. 8. The stochastic simplicial complex of Van der Pol oscillators with $g(x_i) = [0, x_{i2}]^{\mathrm{T}}$, $\omega^{(1)}(x_j) = [x_{j1}^3, x_{j2}^3]^{\mathrm{T}}$, and $\omega^{(2)}(x_j, x_k) = [x_{j1}^2 x_{k1}, x_{j2}^2 x_{k2}]^{\mathrm{T}}$: (a) the largest Lyapunov exponents $\Lambda(\eta, \sigma_v)$, (b) the MSF curves for different noise intensities.

region disappears. Figure 7(b) confirms this observation, where the MSF curve for $\sigma_v = 1.7$ lies above that for $\sigma_v = 2.6$, and the curve for $\sigma_v = 5.1$ surpasses all others except for $\sigma_v = 0.2$, indicating no synchronized region exists. Similar trends are evident in Fig. 8, where $g(x_i) = [0, x_{i2}]^{\mathrm{T}}$, $\omega^{(1)}(x_j) = [x_{j1}^3, x_{j2}^3]^{\mathrm{T}}$, and $\omega^{(2)}(x_j, x_k) = [x_{j1}^2 x_{k1}, x_{j2}^2 x_{k2}]^{\mathrm{T}}$.

Through the above analysis, it can be concluded that when noise affects only a subset of the state variables, its impact on the synchronizability of stochastic simplicial complexes can vary, it may either enhance or hinder synchronization. This variability arises from the complex interplay between the intrinsic dynamics of the nodes, the structure of higher-order interactions, and the coupling strengths in the simplicial complex. In some cases, selective noise can help synchronize specific variables more effectively, improving overall network coherence. However, in other instances, it may introduce imbalances in the system, disrupting the collective dynamics and reducing synchronizability. The outcome largely depends on the type of internal node dynamics and how the noise interacts with both local and global network properties. Thus, the effect of noise on synchronization in such systems is nuanced and context-dependent, requiring a careful examination of the noise diffusion mechanism and the network's structural configuration to predict its overall impact.

4.2. Rössler system

A single Rössler system is described by

$$\begin{aligned} \dot{x}_{i1} &= -x_{i2} - x_{i3}, \\ \dot{x}_{i2} &= x_{i1} + a x_{i2}, \\ \dot{x}_{i3} &= \beta + x_{i3}(x_{i1} - c), \end{aligned} \tag{19}$$

where $a = \beta = 0.2$ and $c = 5.7$. The corresponding Jacobian matrix J_{F} is given by

$$J_{\mathrm{F}} = \begin{bmatrix} 0 & -1 & -1 \\ 1 & a & 0 \\ x_{s3} & 0 & x_{s1} - c \end{bmatrix}. \tag{20}$$

Next, the J_g under different diffusion functions is provided.

(i) Consider the case where the diffusion function $g(x_i) = x_i$. Then

$$J_g = \begin{bmatrix} 1 & 0 & 0 \\ 0 & 1 & 0 \\ 0 & 0 & 1 \end{bmatrix}. \tag{21}$$

The desired state $x_{\mathrm{s}} = [x_{s1}, x_{s2}, x_{s3}]^{\mathrm{T}}$ satisfies the following condition:

$$\begin{bmatrix} \mathrm{d}x_{s1} \\ \mathrm{d}x_{s2} \\ \mathrm{d}x_{s3} \end{bmatrix} = \begin{bmatrix} -x_{s2} - x_{s3} \\ x_{s1} + a x_{s2} \\ \beta + x_{s3}(x_{s1} - c) \end{bmatrix} \mathrm{d}t + \sigma_v \begin{bmatrix} x_{s1} \\ x_{s2} \\ x_{s3} \end{bmatrix} \mathrm{d}W(t). \tag{22}$$

(ii) Consider the case where the diffusion function $g(x_i) = [x_{i1}, x_{i2}, 0]^{\mathrm{T}}$. Then

$$J_g = \begin{bmatrix} 1 & 0 & 0 \\ 0 & 1 & 0 \\ 0 & 0 & 0 \end{bmatrix}. \tag{23}$$

Therefore, the desired state x_{s} satisfies the following condition:

$$\begin{bmatrix} \mathrm{d}x_{s1} \\ \mathrm{d}x_{s2} \\ \mathrm{d}x_{s3} \end{bmatrix} = \begin{bmatrix} -x_{s2} - x_{s3} \\ x_{s1} + a x_{s2} \\ \beta + x_{s3}(x_{s1} - c) \end{bmatrix} \mathrm{d}t + \sigma_v \begin{bmatrix} x_{s1} \\ x_{s2} \\ 0 \end{bmatrix} \mathrm{d}W(t). \tag{24}$$

(ii) Consider the case where the diffusion function $g(x_i) = [0, x_{i2}, 0]^{\mathrm{T}}$. Then

$$J_g = \begin{bmatrix} 0 & 0 & 0 \\ 0 & 1 & 0 \\ 0 & 0 & 0 \end{bmatrix}. \tag{25}$$

The desired state x_{s} satisfies the following condition:

$$\begin{bmatrix} \mathrm{d}x_{s1} \\ \mathrm{d}x_{s2} \\ \mathrm{d}x_{s3} \end{bmatrix} = \begin{bmatrix} -x_{s2} - x_{s3} \\ x_{s1} + a x_{s2} \\ \beta + x_{s3}(x_{s1} - c) \end{bmatrix} \mathrm{d}t + \sigma_v \begin{bmatrix} 0 \\ x_{s2} \\ 0 \end{bmatrix} \mathrm{d}W(t). \tag{26}$$

Next, the $J_{\omega^{(1)}}$ under different inner-coupling functions is provided.

(I) Consider the case where $\omega^{(1)}(x_j) = [x_{j1}^3, 0, 0]^{\mathrm{T}}$ and $\omega^{(2)}(x_j, x_k) = [x_{j1}^2 x_{k1}, 0, 0]^{\mathrm{T}}$. The Jacobian matrix $J_{\omega^{(1)}}$ is given by

$$J_{\omega^{(1)}} = \begin{bmatrix} 3x_{s1}^2 & 0 & 0 \\ 0 & 0 & 0 \\ 0 & 0 & 0 \end{bmatrix}. \tag{27}$$

(II) Consider the case where $\omega^{(1)}(x_j) = [0, x_{j1}^3, 0]^{\mathrm{T}}$ and $\omega^{(2)}(x_j, x_k) = [0, x_{j1}^2 x_{k1}, 0]^{\mathrm{T}}$. The Jacobian matrix $J_{\omega^{(1)}}$ is given by

$$J_{\omega^{(1)}} = \begin{bmatrix} 0 & 0 & 0 \\ 0 & 3x_{s1}^2 & 0 \\ 0 & 0 & 0 \end{bmatrix}. \tag{28}$$

Next, we calculate the largest Lyapunov exponent under different noise intensities σ_v and η for various inner-coupling functions and noise diffusion functions.

Firstly, we analyze how noise intensity affects the synchronizability of the stochastic simplicial complex when noise acts on all state variables of the nodes. Consider the case where $\omega^{(1)}(x_j) = [x_{j1}^3, 0, 0]^{\mathrm{T}}$, $\omega^{(2)}(x_j, x_k) = [x_{j1}^2 x_{k1}, 0, 0]^{\mathrm{T}}$, and $g(x_i) = x_i$. Figure 9(a) presents MSF curves under varying noise intensities $\sigma_v = 0.1, 1.1, 2.5, 3, 5$. It is observed that at $\sigma_v = 1.1$, the MSF curve begins to decrease towards 0. With a further increase in σ_v to 1.2, the MSF curve dips below 0, indicating the potential for achieving synchronization in the stochastic simplicial complex. With the increasing of the σ_v, the MSF curve continues to shift downward, reinforcing enhanced synchronizability at higher noise intensities.

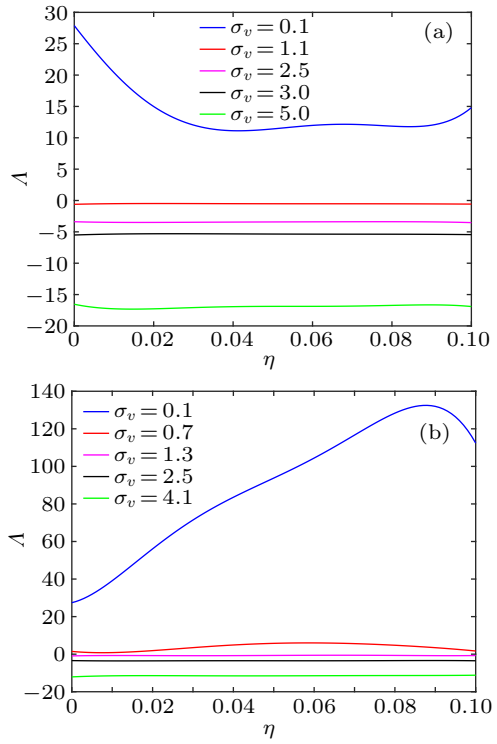


Fig. 9. The MSF curves of the stochastic simplicial complex of Rössler systems under different noise intensities: (a) $g(x_i) = x_i$, $\omega^{(1)}(x_j) = [x_{j1}^3, 0, 0]^{\mathrm{T}}$, and $\omega^{(2)}(x_j, x_k) = [x_{j1}^2 x_{k1}, 0, 0]^{\mathrm{T}}$; (b) $g(x_i) = x_i$, $\omega^{(1)}(x_j) = [0, x_{j1}^3, 0]^{\mathrm{T}}$, and $\omega^{(2)}(x_j, x_k) = [0, x_{j1}^2 x_{k1}, 0]^{\mathrm{T}}$.

Next, we maintain the same diffusion function and analyze a different scenario where the inner-coupling functions are $\omega^{(1)}(x_j) = [0, x_{j1}^3, 0]^{\mathrm{T}}$ and $\omega^{(2)}(x_j, x_k) = [0, x_{j1}^2 x_{k1}, 0]^{\mathrm{T}}$. Figure 9(b) displays the corresponding MSF curves under varying noise intensities $\sigma_v = 0.1, 0.7, 1.3, 2.5, 4.1$. It is evident that for $\sigma_v = 0.1$, the MSF curve remains significantly above zero, suggesting that synchronization is not achievable. However, as σ_v increases to 1.3, the MSF curve begins to decrease towards zero, indicating improved synchronizability. As σ_v continues to rise, the MSF curve shifts further downward, mirroring the behavior seen in the first case, and demonstrating that higher noise intensities generally contribute to enhanced synchronization performance.

Consider a simplicial complex with $\sigma_1 = \sigma_2 = 1$, as shown in Fig. 3. The evolution of the node states with Rössler systems under $\sigma_v = 0$, 0.1, and 3 are illustrated in Figs. 10(a), 10(b), and 10(c), respectively. Here, a synchronization transition phenomenon is still observed. It can be observed that the simplicial complex is unstable under $\sigma_v = 0, 0.1$, while becomes stable under $\sigma_v = 3$ at the desired state. The corresponding system errors are illustrated in Figs. 11(a) and 11(b), respectively. The simulated results are in good agreement with the results in Fig. 9(a).

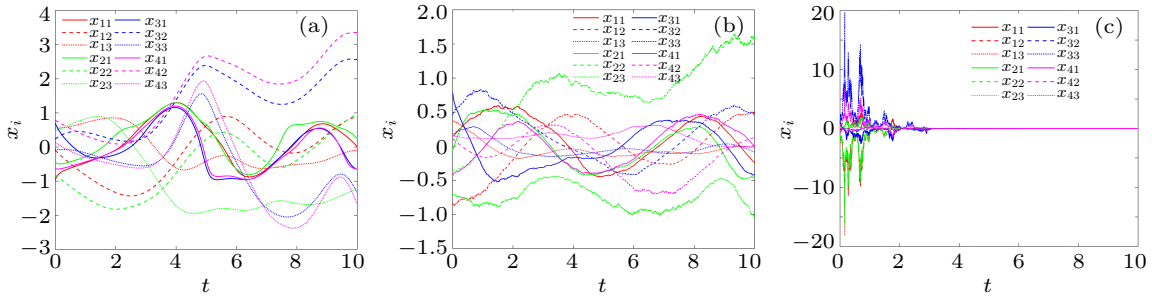


Fig. 10. The evolution of the node states with Rössler systems under different noise intensities: (a) $\sigma_v = 0$, (b) $\sigma_v = 0.1$, and (c) $\sigma_v = 3$.

In both cases, the analysis highlights how increasing noise intensity can lead to enhanced synchronizability when noise affects all state variables of the nodes. The downward shift in the MSF curve as noise intensity increases suggests that, under the right conditions, noise can facilitate synchronization by helping the system overcome local instabilities and reach global coherence.

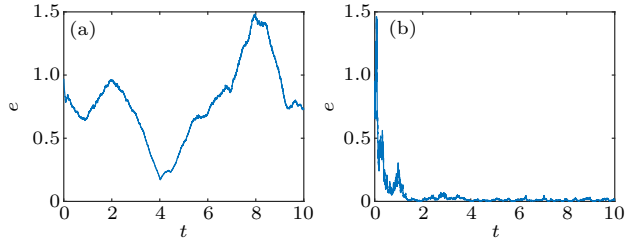


Fig. 11. The evolution of the system errors with Rössler systems under different noise intensities: (a) $\sigma_v = 0.1$ and (b) $\sigma_v = 3$.

In the following, we analyze how the noise intensity affects the synchronizability of simplicial complexes when noise affects only a subset of the node's state variables. Consider the case where $\omega^{(1)}(x_j) = [x_{j1}^3, 0, 0]^{\mathrm{T}}$, $\omega^{(2)}(x_j, x_k) = [x_{j1}^2 x_{k1}, 0, 0]^{\mathrm{T}}$, and $g(x_i) = [x_{i1}, x_{i2}, 0]^{\mathrm{T}}$. Figure 12(a) presents the MSF curves under different noise intensities $\sigma_v = 0.1$, 1.1, 3.6, 4.6, 5.6. It can be observed that for low noise intensities, such as $\sigma_v = 0.1$, the MSF curve remains above zero, indicating that synchronization is unlikely. However, as σ_v increases to 3.6 and beyond, the MSF curve starts to decline, suggesting that synchronization becomes more achievable at higher noise levels. Nevertheless, the effects are not uniform; while synchronizability improves in some cases, further increases from $\sigma_v = 0.1$ in noise intensity (e.g., $\sigma_v = 1.1$) may cause fluctuating results, with the MSF curve showing inconsistent trends.

Next, we examine a different diffusion function, $g(x_i) = [0, x_{i2}, 0]^{\mathrm{T}}$, while keeping the same inner-coupling functions. Figure 12(b) presents the MSF curves under different noise

intensities $\sigma_v = 0.1, 2.1, 2.6, 5.1$. In this scenario, the behavior of the MSF curve similarly reflects the uncertain effects of noise. For $\sigma_v = 0.1$, the MSF curve remains well above zero, indicating weak synchronizability. As noise intensity increases to $\sigma_v = 2.6$, the MSF curve begins to decrease, suggesting improved synchronizability. However, when $\sigma_v = 2.1$, the effect of noise becomes less predictable. While initially shows potential for synchronization, the MSF curve does not continue to follow a consistent downward trend, reflecting the uncertainty in how partial noise propagation affects the network.

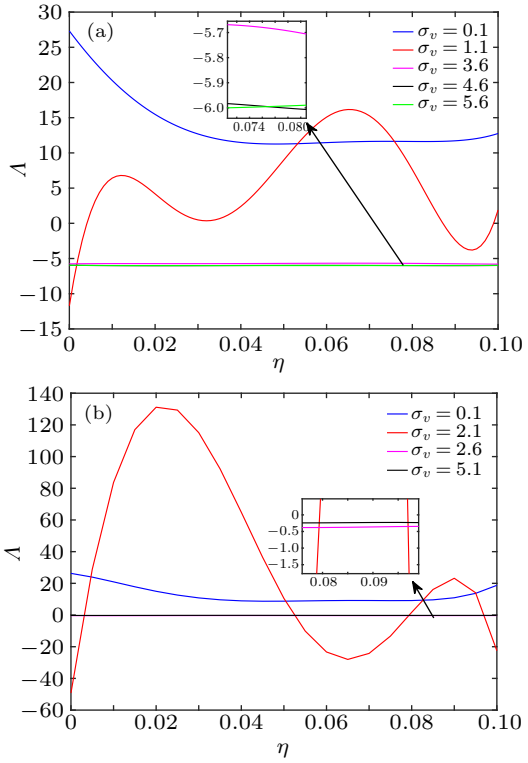


Fig. 12. The MSF curves of the stochastic simplicial complex of Rössler systems under different noise intensities: (a) $g(x_i) = [x_{i1}, x_{i2}, 0]^{\mathrm{T}}$, $\omega^{(1)}(x_j) = [x_{j1}^3, 0, 0]^{\mathrm{T}}$, and $\omega^{(2)}(x_j, x_k) = [x_{j1}^2 x_{k1}, 0, 0]^{\mathrm{T}}$; (b) $g(x_i) = [0, x_{i2}, 0]^{\mathrm{T}}$, $\omega^{(1)}(x_j) = [x_{j1}^3, 0, 0]^{\mathrm{T}}$, and $\omega^{(2)}(x_j, x_k) = [x_{j1}^2 x_{k1}, 0, 0]^{\mathrm{T}}$.

These results demonstrate that when noise influences only a subset of the state variables, its impact on synchronizability becomes more complex and context-dependent. Unlike the case where noise affects all state variables uniformly, selective noise propagation may either improve or hinder synchronization, depending on the interaction between the noise and the network's intrinsic dynamics. This highlights the need for careful analysis of the noise diffusion pattern to accurately assess its influence on the overall performance of the stochastic simplicial complex.

4.3. A simplicial complex

In what follows, we still consider the simplicial complex of four nodes, which has two 2-simplex, as shown in Fig. 3. Consider the case that $\sigma_1 = 0$. Notice that σ_2 is the coupling strength associated with three-body interaction. Figures 13 and 14 depict the largest Lyapunov exponents under varying σ_2 and σ_v. All the results observed in Figs. 2, 6, 7, and 8 can be found in Figs. 13 and 14. When noise affects all state variables of the nodes, increasing noise tends to benefit the

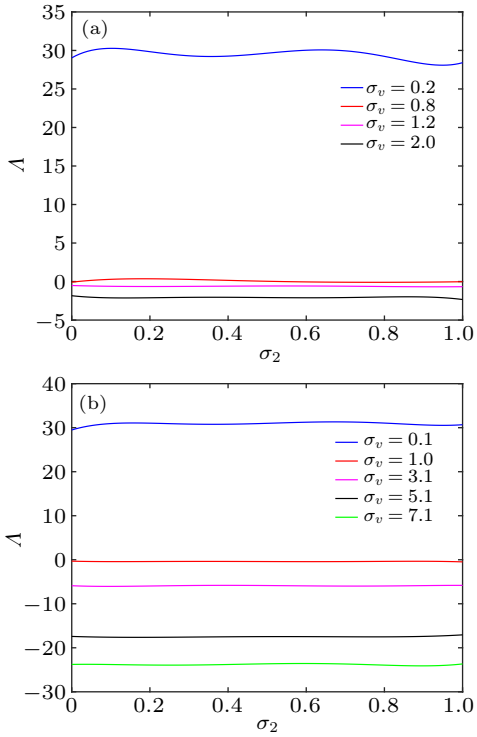


Fig. 13. The MSF curves for the stochastic simplicial complex of Van der Pol oscillators: (a) $g(x_i) = x_i$, $\omega^{(1)}(x_j) = [x_{j1}^3, 0]^{\mathrm{T}}$, and $\omega^{(2)}(x_j, x_k) = [x_{j1}^2 x_{k1}, 0]^{\mathrm{T}}$; (b) $g(x_i) = x_i$, $\omega^{(1)}(x_j) = [x_{j1}^3, x_{j2}^3]^{\mathrm{T}}$, and $\omega^{(2)}(x_j, x_k) = [x_{j1}^2 x_{k1}, x_{j2}^2 x_{k2}]^{\mathrm{T}}$.

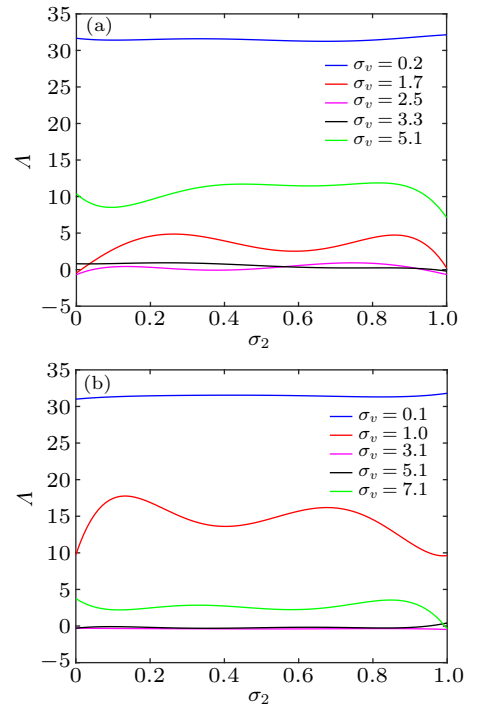


Fig. 14. The MSF curves for the stochastic simplicial complex of Van der Pol oscillators: (a) $g(x_i) = [x_{i1}, 0]^{\mathrm{T}}$, $\omega^{(1)}(x_j) = [x_{j1}^3, 0]^{\mathrm{T}}$, and $\omega^{(2)}(x_j, x_k) = [x_{j1}^2 x_{k1}, 0]^{\mathrm{T}}$; (b) $g(x_i) = [0, x_{i2}]^{\mathrm{T}}$, $\omega^{(1)}(x_j) = [x_{j1}^3, x_{j2}^3]^{\mathrm{T}}$, and $\omega^{(2)}(x_j, x_k) = [x_{j1}^2 x_{k1}, x_{j2}^2 x_{k2}]^{\mathrm{T}}$.

synchronization of simplicial complexes. This may be attributed to the noise introducing a form of "stochastic resonance", where a certain level of noise helps facilitate the collective behavior of the nodes, enhancing their ability to synchronize. On the other hand, when noise affects only a subset of the node's state variables, the effect of increasing noise on synchronizability becomes uncertain. In such cases, the presence of noise may disrupt the delicate balance required for synchronization, leading to inconsistent results that depend heavily on the specific dynamics of the unaffected variables. Further analysis reveals that the interaction between the noise and the specific coupling strengths plays a crucial role in determining the overall stability of the synchronized state. For example, while the higher coupling strength σ_2 generally promotes synchronization, the presence of noise affecting only some nodes can lead to competing dynamics that destabilize the overall system.

In summary, the results highlight the complex interplay between noise, coupling strengths, and the dynamics of the individual nodes in simplicial complexes. This understanding is vital for developing strategies to enhance synchronization in real-world networks, where noise is often unavoidable. Future research could explore adaptive coupling mechanisms or noise mitigation strategies to optimize synchronization in such systems.

5. Conclusion

This paper primarily investigates the synchronization of simplicial complexes under the influence of noise. Firstly, an extended master stability equation and corresponding synchronization stability criteria are provided. Secondly, using Van der Pol oscillators and Rössler systems as the intrinsic dynamics of nodes, the paper delves into how the noise affects the synchronization of simplicial complexes under different noise difussion and inner-coupling functions. The obtained results indicate that the effects of noise on the synchronizability vary with the form of noise propagation. It demonstrates that the presence of noise can regulate the synchronization pattern of the simplicial complex, transforming the unstable state into a stable state, and vice versa. Moreover, the study explores the implications of different coupling configurations in simplicial complexes, demonstrating how varying the strengths and patterns of coupling can either enhance or hinder synchronization in the presence of noise. The analysis includes a comparative examination of different noise propagation mechanisms and their impact on the stability of synchronized states. These findings provide insights and theoretical underpinnings for enhancing the performance of real-world networks, such as social networks, sensor networks, and biological systems, where robust synchronization is essential for functionality. By identifying critical thresholds and optimal coupling strategies, this research contributes to the design of more resilient networked systems that can maintain synchronization despite the inevitable presence of noise. The results pave the way for future studies to explore adaptive control strategies that can mitigate the adverse effects of noise, thereby improving the reliability and efficiency of complex systems in practical applications.

It is worthwhile to mention that, although numerical simulations are performed with two types of nonlinear systems, the extension to other general systems, such as Chen system[48] and Lü system,[49] is straightforward. In the future, exploring the synchronization of higher-order networks with time delay[50–52] would be intriguing. Additionally, addressing synchronization issues in higher-order networks with heterogeneous node dynamics[53,54] and directed topologies,[55] alongside investigating control[56–58] and deep learning[59,60] in higher-order networks, present challenging yet promising avenues for further research.

Appendix A: Proof of Theorem 1

Proof Define $\Delta x_i = x_i - x_{\rm s}$, $i = 1,2,\ldots,N$. The error dynamics is given by

$$\begin{aligned}
{\rm d}\Delta x_i &= {\rm d}x_i - {\rm d}x_{\rm s} \\
&= \Bigg(J_{\rm F}(x_{\rm s})\Delta x_i + \sigma_1 \sum_{j=1}^{N} a_{ij}^{(1)} \Bigg[\frac{\partial H^{(1)}(x_i,x_j)}{\partial x_i}\bigg|_{(x_{\rm s},x_{\rm s})} \Delta x_i \\
&\quad + \frac{\partial H^{(1)}(x_i,x_j)}{\partial x_j}\bigg|_{(x_{\rm s},x_{\rm s})} \Delta x_j \Bigg] \\
&\quad + \sigma_2 \sum_{j=1}^{N}\sum_{k=1}^{N} a_{ijk}^{(2)} \Bigg[\frac{\partial H^{(2)}(x_i,x_j,x_k)}{\partial x_i}\bigg|_{(x_{\rm s},x_{\rm s},x_{\rm s})} \Delta x_i \\
&\quad + \frac{\partial H^{(2)}(x_i,x_j,x_k)}{\partial x_j}\bigg|_{(x_{\rm s},x_{\rm s},x_{\rm s})} \Delta x_j \\
&\quad + \frac{\partial H^{(2)}(x_i,x_j,x_k)}{\partial x_k}\bigg|_{(x_{\rm s},x_{\rm s},x_{\rm s})} \Delta x_k \Bigg] \Bigg) {\rm d}t \\
&\quad + \sigma_v J_g(x_{\rm s})\Delta x_i {\rm d}W(t), \quad i = 1,2,\ldots,N,
\end{aligned} \tag{A1}$$

where $J_{\rm F}(x_{\rm s})$ and $J_g(x_{\rm s})$ are the Jacobian matrices of $F(\cdot)$ and $g(\cdot)$, respectively, at $x_{\rm s}$.

In the following analysis, the local stability of the stochastic simplicial complex is examined. It is noted that all inner-coupling functions are synchronization non-invasive. Consequently, we have $H^{(1)}(x,x) \equiv 0$ and $H^{(2)}(x,x,x) \equiv 0$. At the desired state $x_{\rm s}$, both $H^{(1)}$ and $H^{(2)}$ are constant and equal to zero. Therefore, their total derivatives also vanish.[28,31] Thus, we obtain

$$\begin{aligned}
&\frac{\partial H^{(1)}(x_i,x_j)}{\partial x_i}\bigg|_{(x_{\rm s},x_{\rm s})} + \frac{\partial H^{(1)}(x_i,x_j)}{\partial x_j}\bigg|_{(x_{\rm s},x_{\rm s})} = 0, \\
&\frac{\partial H^{(2)}(x_i,x_j,x_k)}{\partial x_i}\bigg|_{(x_{\rm s},x_{\rm s},x_{\rm s})} + \frac{\partial H^{(2)}(x_i,x_j,x_k)}{\partial x_j}\bigg|_{(x_{\rm s},x_{\rm s},x_{\rm s})}
\end{aligned}$$

$$+\left.\frac{\partial H^{(2)}(x_i,x_j,x_k)}{\partial x_k}\right|_{(x_s,x_s,x_s)}=0,\ \ i=1,2,\ldots,N. \tag{A2}$$

It is well known that

$$\left.\frac{\mathrm{d}H^{(1)}(x_i,x_s)}{\mathrm{d}x_i}\right|_{(x_s)}\Delta x_i=\left.\frac{\partial H^{(1)}(x_i,x_j)}{\partial x_i}\right|_{(x_s,x_s)}\Delta x_i,$$

$$\sum_{j=1}^{N}a_{ij}^{(1)}=k_i^{(1)},\ \ \text{and}\ \ \sum_{j=1}^{N}\sum_{k=1}^{N}a_{ijk}^{(2)}=2k_i^{(2)}=L_{ii}^{(2)}.$$

Substituting Eq. (A2) into Eq. (A1) yields

$$\begin{aligned}\mathrm{d}\Delta x_i=&\Big(J_{\mathrm{F}}(x_{\mathrm{s}})\Delta x_i-\sigma_1\sum_{j=1}^{N}L_{ij}^{(1)}J_{H^{(1)}}(x_s,x_s)\Delta x_j\\&-\sigma_2\sum_{j=1}^{N}L_{ij}^{(2)}[J_{1H^{(2)}}(x_{\mathrm{s}},x_{\mathrm{s}},x_{\mathrm{s}})\\&+J_{2H^{(2)}}(x_{\mathrm{s}},x_{\mathrm{s}},x_{\mathrm{s}})]\Delta x_j\Big)\mathrm{d}t\\&+\sigma_v J_g(x_{\mathrm{s}})\Delta x_i\mathrm{d}W(t),\ \ i=1,2,\ldots,N,\end{aligned} \tag{A3}$$

where

$$\begin{aligned}J_{H^{(1)}}(x_s,x_s)&=\left.\frac{\partial H^{(1)}(x_i,x_j)}{\partial x_j}\right|_{(x_s,x_s)},\\J_{1H^{(2)}}(x_s,x_s,x_s)&=\left.\frac{\partial H^{(2)}(x_i,x_j,x_k)}{\partial x_j}\right|_{(x_s,x_s,x_s)},\\J_{2H^{(2)}}(x_s,x_s,x_s)&=\left.\frac{\partial H^{(2)}(x_i,x_j,x_k)}{\partial x_k}\right|_{(x_s,x_s,x_s)}.\end{aligned}$$

Moreover, $L^{(1)}=(L_{ij}^{(1)})\in\mathbb{R}^{N\times N}$ and $L^{(2)}=(L_{ij}^{(2)})\in\mathbb{R}^{N\times N}$ are the 1-order and 2-order generalized Laplacian matrices, respectively.

It follows from Eqs. (A3), (7), and (8) that

$$\begin{aligned}\mathrm{d}\Delta x_i=&\left(J_{\mathrm{F}}(x_s)\Delta x_i-\sum_{j=1}^{N}\left[\sigma_1L_{ij}^{(1)}+\sigma_2L_{ij}^{(2)}\right]J_{\omega^{(1)}}(x_s)\Delta x_j\right)\mathrm{d}t,\\&+\sigma_vJ_g(x_{\mathrm{s}})\Delta x_i\mathrm{d}W(t),\ \ i=1,2,\ldots,N,\end{aligned} \tag{A4}$$

where $J_{\omega^{(1)}}(x_s)=\left.\frac{\mathrm{d}\omega^{(1)}(x_j)}{\mathrm{d}x_j}\right|_{(x_s)}$.

Let $\Delta x=\left[\Delta x_1^{\mathrm{T}},\Delta x_2^{\mathrm{T}},\ldots,\Delta x_N^{\mathrm{T}}\right]^T\in\mathbb{R}^{mN}$, equation (A4) can be rewritten as

$$\begin{aligned}\mathrm{d}\Delta x=&\left[I_N\otimes J_{\mathrm{F}}-P\otimes J_{\omega^{(1)}}\right]\Delta x\mathrm{d}t\\&+\sigma_vI_N\otimes J_g\Delta x\mathrm{d}W(t),\end{aligned} \tag{A5}$$

where $J_{\mathrm{F}}=J_{\mathrm{F}}(x_{\mathrm{s}})$, $J_g=J_g(x_{\mathrm{s}})$, $J_{\omega^{(1)}}=J_{\omega^{(1)}}(x_{\mathrm{s}})$, $P=\sigma_1L^{(1)}+\sigma_2L^{(2)}$, and I_N is an $N\times N$ identity matrix.

Let $\xi=\left(T^{-1}\otimes I_m\right)\Delta x$. Here, the columns of T are the eigenvectors corresponding to the eigenvalues of P. Then, we have

$$\begin{aligned}\mathrm{d}\xi=&\left[I_N\otimes J_{\mathrm{F}}-U\otimes J_{\omega^{(1)}}\right]\xi\,\mathrm{d}t\\&+\sigma_vI_N\otimes J_g\xi\,\mathrm{d}W(t),\end{aligned} \tag{A6}$$

where $U=\mathrm{diag}(\lambda_1,\lambda_2,\ldots,\lambda_N)$ with $\lambda_1,\lambda_2,\ldots,\lambda_N$ being the eigenvalues of P.

Notice that P is a real symmetric zero-row-sum with eigenvalues $0=\lambda_1<\lambda_2\le\cdots\le\lambda_N$. Equation (A6) can be reformulated as follows:

$$\begin{aligned}\mathrm{d}\xi_i=&\left[J_{\mathrm{F}}-\lambda_iJ_{\omega^{(1)}}\right]\xi_i\mathrm{d}t+\sigma_vJ_g\xi_i\mathrm{d}W(t),\\&i=1,2,\ldots,N.\end{aligned} \tag{A7}$$

Let $\eta=\lambda_i$. Motivated by the MSF formalism,[5] an extended master stability equation is thus obtained as

$$\mathrm{d}y=\left[J_{\mathrm{F}}-\eta J_{\omega^{(1)}}\right]y\mathrm{d}t+\sigma_vJ_gy\mathrm{d}W(t). \tag{A8}$$

It follows from the master stability function approach that the error system (A1) is locally almost sure exponentially stable at zero if the largest Lyapunov exponent calculated by Eq. (A8) is negative. The proof is thus finished.

Remark For $D>2$, $\omega^{(D)}$ satisfies the following conditions:

$$\omega^{(D)}(x,\ldots,x)=\cdots=\omega^{(1)}(x,x)=\omega^{(1)}(x). \tag{A9}$$

Here, the term P in Eq. (A5) for any D can be expressed as

$$P^D=\sigma_1L^{(1)}+\sigma_2L^{(2)}+\cdots+\sigma_DL^{(D)}. \tag{A10}$$

Acknowledgements

Project supported in part by the National Natural Science Foundation of China (Grant Nos. 62473284, 61973064, and 62203327) and Hebei Natural Science Foundation (Grant No. F2022501024).

References

[1] Gao T T, Barzel B and Yan G 2024 *Nat. Commun.* **15** 6029
[2] He M, Chen J, Gong M and Shao Z 2024 *IEEE Transactions on Emerging Topics in Computing* **12** 126
[3] Zheng Q Q, Li X, Shen J W, Pandey V and Guan L N 2024 *J. Phys. A: Math. Theor.* **57** 395203
[4] Boccaletti S, Kurths J, Osipov G, Valladares D and Zhou C 2002 *Phys. Rep.* **366** 1
[5] Pecora L M and Carroll T L 1998 *Phys. Rev. Lett.* **80** 2109
[6] Shi X, Wang Q and Lu Q 2008 *Cognitive Neurodynamics* **2** 195
[7] Han F, Lu Q, Wiercigroch M and Ji Q 2009 *Chin. Phys. B* **18** 482
[8] Del Genio C I, Gómez-Gardeñes J, Bonamassa I and Boccaletti S 2016 *Sci. Adv.* **2** e1601679
[9] Ding L, Yu P, Liu Z W, Guan Z H and Feng G 2013 *Automatica* **49** 2881
[10] Chen F and Chen J 2020 *IEEE Transactions on Automatic Control* **65** 1144
[11] Preciado V M and Rahimian M A 2017 *IEEE Transactions on Network Science and Engineering* **4** 215
[12] Buscarino A, Gambuzza L V, Porfiri M, Fortuna L and Frasca M 2013 *Sci. Rep.* **3** 2026
[13] Wang J, Feng J, Lou Y and Chen G 2021 *IEEE Transactions on Automatic Control* **66** 3267
[14] Xu Y, Wang J, Chen J, Zhao D, Özer M, Xia C and Perc M 2024 *Knowledge-Based Systems* **301** 112326
[15] Fan T, Lü L, Shi D and Zhou T 2021 *Commun. Phys.* **4** 272

[16] Battiston F, Cencetti G, Iacopini I, Latora V, Lucas M, Patania A, Young J G and Petri G 2020 *Phys. Rep.* **874** 1
[17] Ghorbanchian R, Restrepo J G, Torres J J and Bianconi G 2021 *Commun. Phys.* **4** 120
[18] Lucas M, Cencetti G and Battiston F 2020 *Phys. Rev. Res.* **2** 033410
[19] Reitz M and Bianconi G 2020 *J. Phys. A: Math. Theor.* **53** 295001
[20] Reimann M W, Nolte M, Scolamiero M, Turner K, Perin R, Chindemi G, Dłotko P, Levi R, Hess K and Markram H 2017 *Frontiers in Computational Neuroscience* **11** 48
[21] Majhi S, Perc M and Ghosh D 2022 *Journal of the Royal Society Interface* **19** 20220043
[22] Dai X, Kovalenko K, Molodyk M, Wang Z, Li X, Musatov D, Raigorodskii A, Alfaro-Bittner K, Cooper G, Bianconi G, *et al.* 2021 *Chaos, Solitons & Fractals* **146** 110888
[23] Zomorodian A and Carlsson G 2005 *Discrete & Computational Geometry* **33** 249
[24] Sizemore A E, Giusti C, Kahn A, Vettel J M, Betzel R F and Bassett D S 2018 *J. Comput. Neurosci.* **44** 115
[25] Shi D, Lü L and Chen G 2019 *National Science Review* **6** 962
[26] Shi D, Chen Z, Sun X, Chen Q, Ma C, Lou Y and Chen G 2021 *Commun. Phys.* **4** 249
[27] Courtney O T and Bianconi G 2016 *Phys. Rev. E* **93** 062311
[28] Gambuzza L V, Di Patti F, Gallo L, Lepri S, Romance M, Criado R, Frasca M, Latora V and Boccaletti S 2021 *Nat. Commun.* **12** 1255
[29] Anwar M S and Ghosh D 2022 *Phys. Rev. E* **106** 034314
[30] Gallo L, Muolo R, Gambuzza L V, Latora V, Frasca M and Carletti T 2022 *Commun. Phys.* **5** 263
[31] Gambuzza L V, Di Patti F, Gallo L, Lepri S, Romance M, Criado R, Frasca M, Latora V and Boccaletti S 2022 *Higher-Order Systems* (Springer) pp. 249–267
[32] Chen G 2022 *IEEECAA Journal of Automatica Sinica* **9** 573
[33] Shi D and Chen G 2022 *National Science Review* **9** nwac038
[34] Wang Y and Zhao Y 2024 *Chaos, Solitons and Fractals* **185** 115062
[35] Gao Z, Ghosh D, Harrington H A, Restrepo J G and Taylor D 2023 *Chaos* **33** 040401
[36] Chen J, Sun S, Xia C, Shi D and Chen G 2023 *IEEE Transactions on Network Science and Engineering* **10** 3767
[37] Chen J, Xia C and Perc M 2024 *IEEE Transactions on Computational Social Systems* **11** 4267
[38] Hu J, Wu Y, Li T and Ghosh B K 2019 *IEEE Transactions on Automatic Control* **64** 2122
[39] Wu Y, Liang Q, Zhao Y, Hu J and Xiang L 2021 *European Journal of Control* **59** 123
[40] Wang G, Cao J and Lu J 2010 *Physica A* **389** 1480
[41] Zhou C and Kurths J 2002 *Phys. Rev. Lett.* **88** 230602
[42] Sun J, Xiang L and Chen G 2023 *Frontiers in Physics* **11** 112984
[43] Porfiri M and Frasca M 2019 *IEEE Transactions on Control of Network Systems* **6** 375
[44] Yan X, Li Z and Li C 2024 *Chin. Phys. B* **33** 028705
[45] Russo G and Shorten R 2018 *Physica D* **369** 47
[46] Rossa F D and DeLellis P 2020 *Phys. Rev. E* **101** 052211
[47] Duolan, Xiang L and Chen G 2023 *Chin. Phys. B* **32** 060502
[48] Chen G and Ueta T 1999 *Int. J. Bifurc. Chaos* **9** 1465
[49] Lü J and Chen G 2002 *Int. J. Bifur. Chaos* **12** 659
[50] Guo Z H, Li Z J, Wang M J and Ma M L 2023 *Chin. Phys. B* **32** 038701
[51] Zhu C, Zhang P, Lu Z, Yang B and Wang Z 2023 *Proceedings of the Institution of Mechanical Engineers, Part I: Journal of Systems and Control Engineering* **238** 112
[52] Chen F, Chen X, Xiang L and Ren W 2021 *Automatica* **123** 109356
[53] Rakshit S and Pasqualetti F 2023 *IEEE Control Systems Letters* **7** 3259
[54] Chen F, Feng G, Liu L and Ren W 2015 *IEEE Transactions on Automatic Control* **60** 547
[55] De Lellis P, Della Rossa F, Lo Iudice F and Liuzza D 2023 *IEEE Control Systems Letters* **7** 691
[56] Xia R and Xiang L 2024 *European Journal of Control* **77** 100994
[57] Zhou J, Li B, Lu J A and Shi D 2024 *Scientia Sinica Informationis* **54** 708
[58] Xie X, Zhou Q, Yue D and Li H 2018 *IEEE Transactions on Systems, Man, and Cybernetics: Systems* **48** 2251
[59] Wang Z, Yang K, Li L, Lu Y and Tao Y 2023 *IET Intelligent Transport Systems* **17** 1363
[60] Hu Y, Fu J and Wen G 2023 *IEEE Transactions on Intelligent Vehicles* **8** 2332